NANOCIÊNCIAS E NANOTECNOLOGIA:

Pesquisa e Aplicações

Juan Ramón Collet-Lacoste
(Organizador)

EDITORA ARTEMIS
2022

NANOCIÊNCIAS E NANOTECNOLOGIA:

Pesquisa e Aplicações

Juan Ramón Collet-Lacoste
(Organizador)

EDITORA ARTEMIS
2022

Editora Chefe	Profª Drª Antonella Carvalho de Oliveira
Editora Executiva	M.ª Viviane Carvalho Mocellin
Direção de Arte	M.ª Bruna Bejarano
Diagramação	Elisangela Abreu
Organizador	Prof. Dr. Juan Ramón Collet-Lacoste
Imagem da Capa	Liuzishan/123RF
Bibliotecária	Janaina Ramos – CRB-8/9166

Editora Artemis
Curitiba-PR Brasil
www.editoraartemis.com.br
e-mail:publicar@editoraartemis.com.br

Editora Artemis
Curitiba-PR Brasil
www.editoraartemis.com.br
e-mail:publicar@editoraartemis.com.br

Dados Internacionais de Catalogação na Publicação (CIP)

N186 Nanociências e nanotecnologia: pesquisa e aplicações / Organizador Juan Ramón Collet-Lacoste. – Curitiba-PR: Artemis, 2022.

Formato: PDF
Requisitos de sistema: Adobe Acrobat Reader
Modo de acesso: World Wide Web
Inclui bibliografia
ISBN 978-65-87396-66-8
DOI 10.37572/EdArt_290822668

1. Nanociência. 2. Nanotecnologia. 3. Pesquisa. I. Collet-Lacoste, Juan Ramón (Organizador). II. Título.

CDD 620.5

Elaborado por Bibliotecária Janaina Ramos – CRB-8/9166

EDITORA ARTEMIS
2022

Editora Artemis
Curitiba-PR Brasil
www.editoraartemis.com.br
e-mail:publicar@editoraartemis.com.br

PRÓLOGO

Las propiedades particulares de las Nps, muy diferentes en muchos aspectos a las de sus sólidos masivos, han abierto nuevos campos de estudio e investigación a todo nivel: teóricos y aplicados. Son más inestables que los sólidos masivos de los que se diferencian principalmente por su estructura electrónica que no suele ser continua. Esto es una ventaja a nivel de su reactividad y suelen presentar superficies específicas altas que son muy propicias para los procesos de catálisis, un ingrediente muy importante en los procesos cinéticos. Otra propiedad interesante es que no presentan defectos estructurales en su volumen como vacancias o dislocaciones, a diferencia de sus correspondientes sólidos masivos.

Las presentes monografías forman parte del título: "Nanociências e Nanotecnologia: Pesquisa e Aplicações". Los artículos están ordenados de lo más general (*e.g.*, producción y caracterización de las Nps) a los relacionados con aplicaciones prácticas (*e.g.*, foto catálisis y a su relación principalmente con aplicaciones de origen biológico).

Estos muestran la potencialidad de las nanotecnologías en la comprensión de nuevas aplicaciones en campos tan variados como la catálisis, fotocatálisis, bio-remediación, contaminantes, ambientes acuáticos, antisépticos, bactericidas, virucidas, compuestos bio-activos, biosíntesis extracelular e intracelular, estudio de suelos, vegetales y probióticos, etc.

Juan Ramón Collet-Lacoste

SUMÁRIO

CAPÍTULO 6

COMPLEX OXIDATION OF TMB CATALYZED WITH PEROXIDASE-LIKE AU NANOPARTICLES[1]

Data de submissão: 19/05/2022
Data de aceite: 10/06/2022

Zhiming Liu
Academy of Chemical Defense
Academy of Military Science
Beijing, China
https://orcid.org/0000-0003-1819-7967

Wenjian Wu
College of Science
National University of
Defense Technology
Changsha, China

ABSTRACT: Metal nanoparticles with catalytic properties are very promising to be used as detectors in biochemical reactions. Herein reveals the catalytic properties and relevant *in-situ* self-assembly abilities of hybrid films of Au nanoparticles (Au NPs) and cellulose for the oxidation of benign chromogen 3,3',5,5'-tetramethylbenzidine (TMB) with hydrogen peroxide (H_2O_2). The peroxidase-like properties of hybrid films are inherited from those of colloidal Au NPs and increase with their contents of Au NPs. It is discovered that the oxidized products of TMB grow *in-situ* and assemble into rod-like and tumbleweed-like nanofiber assemblies on hybrid films. The rod-like nanofibers show a magnificent polarizing phenomenon under polarized light because of polycrystalline globular nanoparticles inside. The *in-situ* self-assembly of polarizing nanofibers of chromogen catalyzed with hybrid films creates an opportunity for the synthesis of novel organic nanomaterials and the enhanced detection of biochemical products under polarized light.

KEYWORDS: Self-Assembly. Nanofiber. Tetramethylbenzidine. Hybrid Film. Au Nanoparticle.

1 INTRODUCTION

Historically, gold (Au) has been regarded as being catalytically inert. However, it is surprisingly discovered that Au NPs with either positive or negative surface charges show peroxidase-like activity to H_2O_2 in the presence of TMB [1-3], which has a stronger affinity to negatively charged surfaces of Au NPs [2]. It is revealed that the origin of the peroxidase-like activity seen from Au NPs is contributed by the Au NPs [3], and the Au NPs is 55 times less active than the native enzyme [4]. Although Au NPs are observed to enhance the activities of glucose oxidase and horseradish peroxidase (HRP) [5, 6], and some

[1] Originally Published: Nanotechnology, 2017, 28, 385602 (7pp).

of them even possess intrinsic peroxidase [3-6], there are not any reports about hybrid materials of Au NPs being used directly as catalysts of H_2O_2 for the oxidation of organic chromogens such as TMB. As a non-carcinogenic compound, TMB has been widely used as a new reagent for swift colorimetric detection of biomolecules in analytical samples [7-9]. The self-assembly and transformation of nanostructures is found to be controlled by enzymatic kinetics in a system consisting of HRP, H_2O_2, and TMB [10]. Furthermore, these complex nanofibers of oxidized TMB are expected to have wide applications in organic electronics and photonic devices [11-16]. Meanwhile, compared with the enzyme-controlled self-assembly approach which has attracted considerable attention of scientists [10, 17], hybrid materials with enzyme-like catalytic properties are more promising for synthesizing novel smart materials with controlled nanostructures because of the *in-situ* catalyzing ability, easy separation from solutions, and wide adaptability to chemical reagents, *etc*.

2 EXPERIMENTAL DETAILS

Herein, catalytic properties of hybrid films of Au NPs and cellulose to H_2O_2 for the oxidation of TMB are studied. The oxidized products of TMB can grow *in-situ* on the hybrid films and assemble into structures with different morphologies, including both straight and curved rod-like nanofibers, tumbleweed-like nanofiber assemblies, and polycrystalline straw-berry-like nanoparticles within rod-like nanofibers. The rod-like nanofibers exhibit glorious polarizing phenomenon because of polycrystalline characteristics of the globular nanoparticles inside.

Two kinds of Au colloids with average sizes of Au NPs around 13 nm (abbreviated Au13) and 50 nm (abbreviated Au50) under transmission electron microscope (TEM, JEOL JEM 1400 EX, 120 keV) are prepared by the citrate reduction of $HAuCl_4$. The Au colloids of Au13 and Au50 exhibit characteristic surface plasmon resonance (SPR) bands centered at 520 nm and 547 nm under UV-Vis spectrometer (Perkin-Elmer Lambda II), respectively. Dynamic light scattering (DLS, Malvern Zetasizer Nano-ZS) tests show that Zeta potentials of both the Au NPs of Au13 and Au50 are negatively charged, and their average hydrodynamic sizes are larger than those tested under TEM.

100 μL Au13 (0.209 mg/mL) or Au50 (0.511 mg/mL) is added into 1 mL TMB reaction solution composed of 0.42 mM TMB and 10 mM H_2O_2 in an aqueous sodium phosphate citrate buffer with pH of 5.0 to initiate the redox reaction at room temperature for 24 h. The suspension is centrifuged under 13 krpm for 20 min to precipitate Au NPs after the reaction. The supernatant is tested with UV-Vis spectrometer. 10 μg/mL HRP is used as a contrast of Au colloid to catalyse the oxidation of TMB and the 10-fold dilution

of the resulting solution is tested for contrast. In a TMB/HRP/H_2O_2 system, the first blue product of oxidized TMB is TMB^+ which is the protonated cation of TMB diamine with major absorbance peaks at 370 and 652 nm (exhibiting a blue color), and the final product is TMB^{2+} which is the protonated dication of TMB diimine with maximum absorbance at 450 nm (exhibiting a yellowish color) [18, 19]. And TMB diamine is in equilibrium with CTC which is the complex of TMB and TMB diimine.

3 RESULTS AND DISCUSSIONS

The absorbance peaks of oxidized TMB catalyzed with Au NPs around 370 nm, 450 nm and 652 nm indicate the presence of both CTC and TMB diimine in the product (**Figure 1a**). Au NPs of both Au13 and Au50 show peroxidase-like catalytic properties to TMB in the reaction solution, although their activities are much lower than that of HRP. Hybrid films with 3.0%, 6.5%, 13.7% and 20.6% Au13 and hybrid films with 4.9%, 9.5%, 12.8%, 14.5% and 23.2% Au50 (mass contents in weight) are synthesized according to the method published before [20, 21]. As to verify the peroxidase-like properties of hybrid films with Au13 and Au50, pieces of these two kinds of hybrid films with different wet mass in each group (5 mg for hybrid films with Au13 and 8.5 mg for hybrid films with Au50) are used to test their catalytic properties to TMB. And a piece of pure cellulose film without Au NPs is applied as control. The testing method of hybrid films is the same as that of Au NPs except there is no need to centrifuge the resulting solution to remove hybrid films.

The CTC characteristic absorbance of blue reaction solution increases with the concentration of Au NPs of hybrid films with Au13 (**Figure 1b**) or Au50 (**Figure 1c**). It reveals the peroxidase-like property of hybrid films is inherited from Au NPs and hydrated Au NPs in the hybrid films are incorporated in the catalytic processes, since there is no significant characteristic absorbance of oxidized TMB produced when the pure cellulose film is applied. The catalytic activity of hybrid film is quantified by the characteristic absorbance at 652 nm normalized with the dry mass of each hybrid film (**Figure 1c**).

Hybrid films with Au13 show much higher catalytic activities compared with hybrid films with Au50 (**Figure 1d**). It indicates hybrid films with smaller Au NPs will exhibit higher catalytic activities compared with those of hybrid films with larger Au NPs even when they have the same mass content of Au NPs. And this phenomenon is in accordance with the fact that the catalytic activity may be related with the surface area of Au NPs of a hybrid film, since the surface area of Au NPs of a hybrid film with small Au NPs is larger than that with large Au NPs. When the size of Au NPs changes from 50 nm to 13 nm, the

surface area of Au NPs increases 3.85 folds as to their relevant hybrid films with the same mass content of Au NPs. However, although the catalytic activity of hybrid film with 13.7% Au13 is 1.8 folds higher than that of hybrid film with 14.5% Au50, it seems that the increase of catalytic efficiency is not as high as predicted.

Since it is revealed that the superficial Au atoms are a contributing factor to the observed peroxidase-like activity of Au NPs [6], the phenomenon above may be caused by the relative decrease of superficial atoms with effective catalytic properties as to the hybrid films with fewer and larger Au NPs. The dehydration of hybrid films is conducted to obtain dry hybrid films to examine their peroxidase-like properties in different physical states, by drying wet hybrid films on plastic Petri dishes in air at room temperature and 50% moisture for 24 hours. It is very interesting that the dehydration of hybrid films depletes their peroxidase-like properties and leave the relevant reaction solutions clear because of the dehydration of Au NPs of dry hybrid films (**inset in Figure 1d**).

Figure 1. (a) UV-Vis spectra of TMB reaction solutions with different catalysts. (b) Absorbance spectra of TMB reaction solutions catalyzed by hybrid films with different contents of Au13 compared with that cultured with a cellulose film. (c) Absorbance spectra of TMB reaction solutions catalyzed by hybrid films with different contents of Au50 compared with that cultured with a cellulose film. (d) Comparison of peroxidase-like activities of hybrid films with Au13 and Au50 (with a starting point of cellulose film). The inset in part (d) illustrated the TMB reaction solutions with hybrid films in dry physical states.

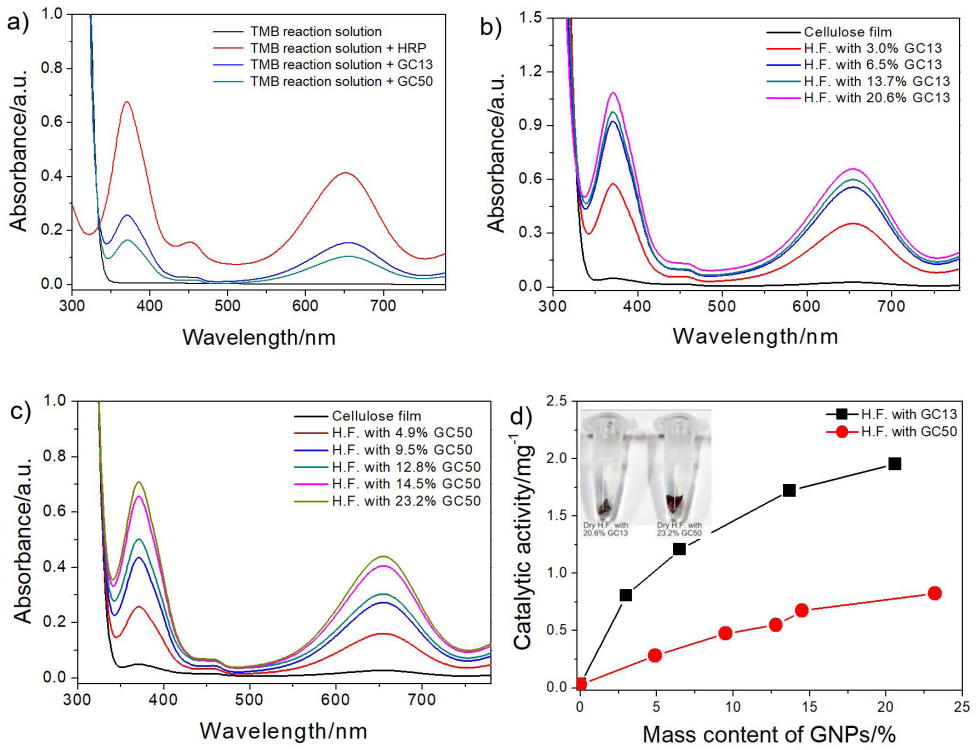

Although the hybrid films with 20.6% Au13 or 23.2% Au50 have the highest concentration of Au NPs and catalytic activities in their corresponding groups of hybrid films, their relevant dry films don't show any peroxidase-like properties in TMB reaction solutions. The phenomenon above may be caused by the valence changes of superficial atoms on Au NPs during the dehydration process which embodies metal-like properties to the closely packed Au NPs of dry hybrid films. However, it's very attractive that the peroxidase-like property of wet hybrid films maintains after rinsing the wet hybrid films with deionized H_2O thoroughly.

It is discovered that the oxidized products of TMB assemble *in-situ* and grow into nanofibers on hybrid films when the reaction solutions are kept still for 24h at room temperature. However, the self-assembly phenomenon is not observed in the TMB reaction solutions catalyzed by HRP, Au13 or Au50 (relevant with **Figure 1a**). It confirms the exclusive role of Au NPs assembled on the surface of hybrid film in the formation of fibrous TMB products. The existence of fibrous products of oxidized TMB is very obvious in TMB reaction solutions catalyzed by hybrid films with Au13. The amount of fibrous products seems increasing with the contents of Au NPs of hybrid films. And the decreasing blue color of TMB reaction solutions also reveals the assembly of oxidized TMB catalyzed by hybrid films with higher content of Au13 is more complete. However, the existence of fibrous products in TMB reaction solutions catalyzed by hybrid films with Au50 is not significant, which should be responsible for the obvious blue color of their relevant TMB reaction solutions. The assembly and growth of fibrous products on hybrid films is greatly influenced by both size and content of Au NPs in hybrid films.

There are two kinds of fibrous products of oxidized TMB formed on the surface of hybrid film with 20.6% Au13 (**Figure 2a**). One is rod-like nanofibers, and the other is tumbleweed-like assemblies. The rod-like nanofibers root on the hybrid film, which should be the result of *in-situ* self-assembly of oxidized TMB on the surfaces of Au NPs in hybrid films. Meanwhile, the bare surface of cellulose film (**inset in Figure 2a**) cultured in TMB reaction solution convinces that fibrous products formed on surfaces of hybrid films are catalyzed by Au NPs of hybrid films. Cellulose in hybrid films is just the supporting matrix of Au NPs and it is not involved in the formation of fibrous TMB products. Meanwhile, the tumbleweed-like assemblies with an average diameter around 140 μm are not localized on the hybrid films and some of them are not fully developed into globular structures. The red color of hybrid film with 20.6% Au13 originates from the characteristic surface plasma resonance bands of Au NPs in the hybrid film [18].

It is discovered for the first time that rod-like nanofibers extended from the hybrid film show a magnificent polarization phenomenon under polarized light which enhances

their visibility greatly (**Figure 2b**). Fibrous products of oxidized TMB are separated from hybrid films in a process of shaking the Eppendorf tube containing TMB reaction solutions, picking out bare hybrid films, centrifuging and transferring the sediment of fibrous products into deionized water. The maximal length of rod-like nanofibers is more than 1 mm (**Figure 2c**), which is above the length scale of nanobelts precipitated out of the solution of TMB/HRP/H_2O_2 system [10]. The nanofibers exhibit a green color under nonpolarized light (**Figure 2c**) indicating they are composed of both blue CTC and yellow TMB diamine [20, 21]. The shinning rod-like nanofibers under polarized light reveals their crystalline characteristics. However, the tumbleweed-like nanofiber assemblies show a deep blue color (**Figure 2c**) and don't exhibit any polarization phenomenon under polarized light (**Figure 2d**), revealing the tumbleweed-like nanofiber assemblies should be composed of amorphous CTC of TMB only. It is in accordance with the assumption that nanobelts precipitated out of the solution of TMB/HRP/H_2O_2 system are composed of CTC of TMB [10]. So, the TMB diimine which is the other oxidized product of TMB in rod-like nanofibers should be in the form of crystalline substance.

Figure 2. (a) Optical image of fibrous products of oxidized TMB rooted on hybrid film with Au13. The inset in part (a) illustrates the bare cellulose film cultured in TMB reaction solution with a scale bar of 200 μm. (b) Optical image of rod-like nanofibers extended from the hybrid film with Au13 under polarized light. (c) Optical image of green rod-like nanofibers and a tumbleweed-like assembly with a deep blue color. (d) Optical image of shinning rod-like nanofibers and a dark tumbleweed-like assembly under polarized light.

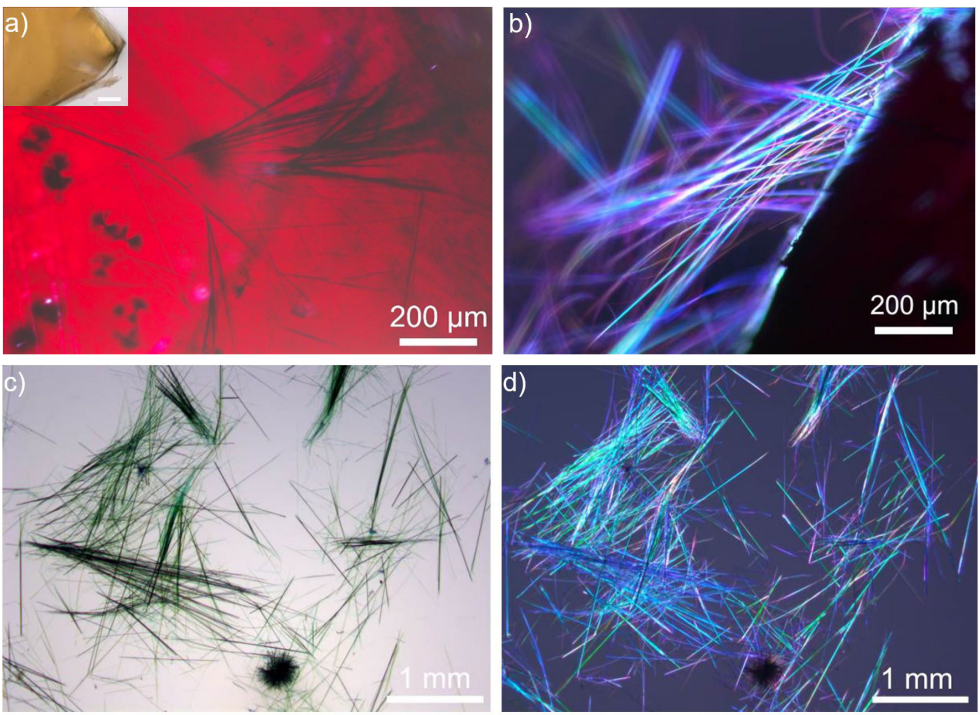

Scanning electron microscopy (SEM, JEOL IT 300, 10 kV) images of the fibrous products not only confirm the existence of rod-like (**Figure 3a**) and tumbleweed-like (**Figure 3b**) fibrous products of oxidized TMB, but also reveal the growing process of these two kinds of nanofibers (**Figure 3c and 3d**). Although the rod-like nanofibers are very straight and separated from each other in their upside parts, the bound and curled morphology of their root areas indicate they are confined on the surfaces of hybrid films at the beginning of their growth (**Figure 3c**). The undeveloped tumbleweed-like nanofiber assemblies show that they are assembled by separate nanofibers tangled together in their root areas (**Figure 3d**). TEM images of the nanofibers reveal their inner structures (**Figure 3e**). There are globular nanoparticles assembled into the rod-like nanofibers. And the globular nanoparticles show unique surfaces of strawberry-like morphologies (**Figure 3f**). The inhomogeneous morphologies of globular nanoparticles are very different from their analogies of nanoparticles formed in the solution of TMB/HRP/H_2O_2 system at high HRP concentrations [10]. It may be attributed to the compositional difference in these two kinds of nanoparticles, with the former strawberry-like nanoparticles being composed of diimine and the latter being composed of azo dimer, because of the weaker catalyzing ability of hybrid films compared with that of HRP.

Figure 3. (a) SEM image of tumbleweed-like nanofiber assemblies. (b) SEM image of rod-like nanofibers. (c) SEM image of the root area of rod-like nanofibers. (d) SEM image of an undeveloped tumbleweed-like nanofiber assembly. (e) TEM image of rod-like nanofibers with nanoparticles inside. (f) TEM image of a strawberry-like nanoparticle.

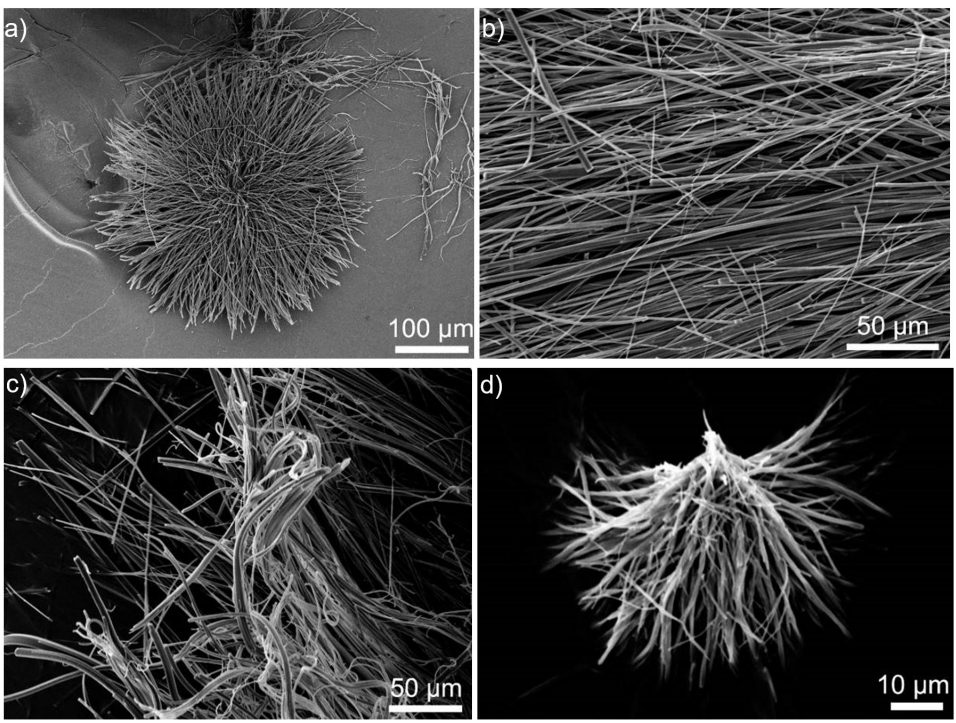

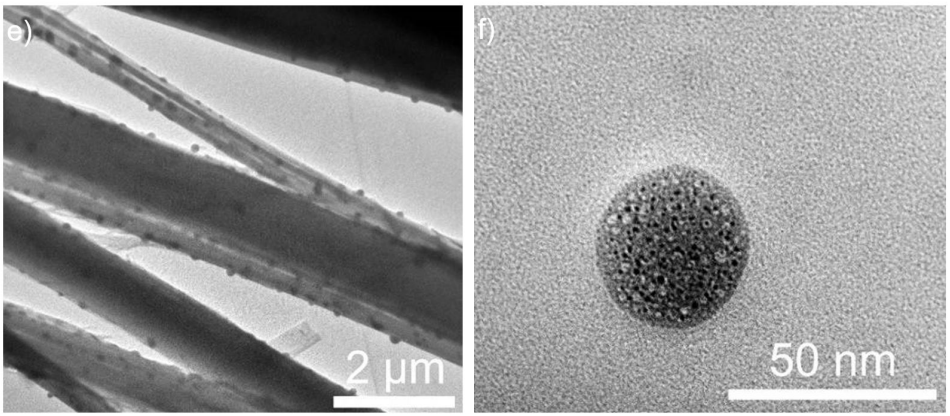

The diameter of globular nanoparticles ranges from 6 nm to 120 nm (**Figure 4a**). The selected area electron diffraction (SAED) patterns confirm the polycrystalline properties of these nanoparticles (**Figure 4b**). A close examination of the rings show that they consisted a large number of spots, each arising from Bragg reflection from an individual crystallite. The interplanar spacing of the three inner rings of **Figure 4d** is 0.0486 nm, 0.0417 nm and 0.0307 nm, respectively, being more than 20 times less than that of the crystal data of 4,4'-Diamino-2,2',6,6'-tetramethylbiphenyl which is an isomer of TMB [24].

Figure 4. (a) TEM image of rod-like nanofibers with nanoparticles inside. (b) SAED image of the globular nanoparticles in part (a) (For recording purposes, the central diffraction spot is masked by a wire).

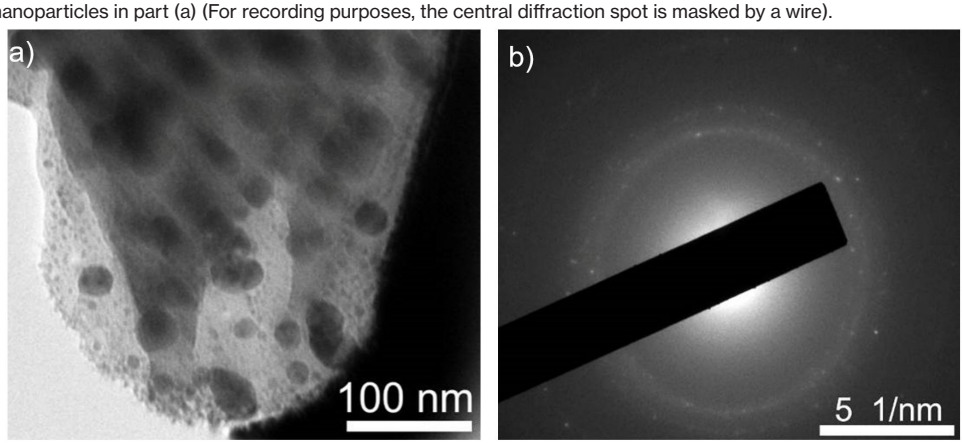

So, there is a hypothesis that the polycrystalline nanoparticles have high-index surfaces and exhibit ordered defects on their surfaces because of the molecular lattice distortion. However, there isn't any significant electron diffraction pattern observed from the outer layers of these nanofibers, indicating the nanofibers are composed of

both amorphous substances and polycrystalline nanoparticles. Comparisons of Fourier transform infrared spectrometer (FTIR, Perkin-Elmer SpectrumTM 100 spectrometer) positions of the most intense peaks of TMB, TMB^{+}, TMB^{2+} [22, 23] and the fibrous products and nuclear magnetic resonance (NMR, Agilent 100/54/ASP spectrometer operating at 400 MHz)) positions verifies that the fibrous products are composed of both CTC and TMB diamine. The results above further reveal that CTC of TMB forms the amorphous nanobelts and TMB diimine forms the polycrystalline nanoparticles.

4 CONCLUSION

In summary, it is discovered for the first time that the oxidized products of TMB can grow and assemble *in-situ* into fibers with unique structures on the surface of hybrid film of Au NPs and cellulose. The rod-like nanofibers show a significant polarizing phenomenon under polarized light. The rod-like nanofibers are proposed to be complex assemblies of amorphous CTC and polycrystalline globular nanoparticles of TMB diimine, and the excess amount of CTC forms tumbleweed-like nanofiber assemblies. The catalytic properties of hybrid films are not only helpful to the oxidation of reducing chemicals, but also providing a unique *in-situ* self-assembly environment for the products because of their high concentrations around Au NPs of hybrid films. This tactic can be applied to the self-assembly of nanostructures with multiple compositions and complex inner structures and it creates opportunities for the enhanced detection of biochemical products under polarized light also.

REFERENCES

[1] X.-X. Wang, Q. Wu, Z. Shan and Q.-M. Huang 2011 BSA-stabilized Au clusters as peroxidase mimetics for use in xanthine detection. *Biosens. Bioelectron.* **26**, 3614-9.

[2] F. Yu, Y. Huang, A. J. Cole and V. C. Yang 2009 The artificial peroxidase activity of magnetic iron oxide nanoparticles and its application to glucose detection. *Biomaterials* **30**, 4716-22.

[3] S. Wang, W. Chen, A.-L. Liu, L. Hong, H.-H. Deng and X.-H. Lin 2012 Comparison of the peroxidase-like activity of unmodified, amino-modified, and citrate-capped gold nanoparticles. *ChemPhysChem* **13**, 1199-204.

[4] H. Wei and E. Wang 2013 Nanomaterials with enzyme-like characteristics (nanozymes): next-generation artificial enzymes. *Chem. Soc. Rev.* **42**, 6060-93.

[5] P. Pandey, S. P. Singh, S. K. Arya, V. Gupta, M. Datta, S. Singh and B. D. Malhotra 2007 Application of thiolated gold nanoparticles for the enhancement of glucose oxidase activity. *Langmuir* **23**, 3333-7.

[6] D. Lan, B. Li and Z. Zhang 2008 Chemiluminescence flow biosensor for glucose based on gold nanoparticle-enhanced activities of glucose oxidase and horseradish peroxidase. *Biosens. Bioelectron.* **24**, 934-8.

[7] B. Li, Y. Du, T. Li and S. Dong 2009 Investigation of 3,3',5,5'-tetramethylbenzidine as colorimetric substrate for a peroxidatic DNAzyme. *Anal. Chim. Acta* **651**, 234-40.

[8] P. Ni, Y. Sun, H. Dai, J. Hu, S. Jiang, Y. Wang and Z. Li 2015 Highly sensitive and selective colorimetric detection of glutathione based on Ag [I] ion-3,3',5,5'-tetramethylbenzidine (TMB). *Biosens. Bioelectron.* **63**, 47-52.

[9] R. P. Alves-Balvedi, L. P. Caetano, J. M. Madurro and A. G. Brito-Madurro 2016 Use of 3,3',5,5' tetramethylbenzidine as new electrochemical indicator of DNA hybridization and its application in genossensor. *Biosens. Bioelectron.* **85**, 226-31.

[10] L. Gao, J. Wu and Di Gao 2011 Enzyme-controlled self-assembly and transformation of nanostructures in a tetramethylbenzidine/horseradish peroxidase/H_2O_2 system. *ACS Nano* **5**, 6736-42.

[11] H. Awano and H. Ohigashi 1989 Electrodeposition of the cationic radical salt of 3,3',5,5'-tetramethylbenzidine. *Synth. Met*. **32**, 389-94.

[12] H. Awano, H. Murakami, T. Yamashita and H. Ohigashi 1991 Electro-deposition of the cationic radical salts of some aromatic diamines from acetonitrile solution. *Synth. Met.* **39**, 327-41.

[13] N. D. Luong, J. Oh, Y. Lee, J. Huh, J. J. Park, J. M. Kim and J.-D. Nam 2011 Self-assembled tetramethylbenzidine conductive nanofibers synchronized with gold nanoparticle formation. *Appl. Surf. Sci.* **257**, 3233-5.

[14] H. Liu, Q. Zhao, Y. Li, Y. Liu, F. Lu, J. Zhuang, S. Wang, L. Jiang, D. Zhu, D. Yu and L. Chi 2005 Field emission properties of large-area nanowires of organic charge-transfer complexes. *J. Am. Chem. Soc.* **127**, 1120-1.

[15] Y. Liu, Z. Ji, Q. Tang, L. Jiang, H. Li, M. He, W. Hu, D. Zhang, L. Jiang, X. Wang, C. Wang, Y. Liu and D. Zhu 2005 Particle-size control and patterning of a charge-transfer complex for nanoelectronics. *Adv. Mater.* **17**, 2953-7.

[16] Y. Li, T. Liu, H. Liu, M.-Z. Tian and Y. Li 2014 Self-assembly of intramolecular charge-transfer compounds into functional molecular systems. *Acc. Chem. Res.* **47**, 1186-98.

[17] R. J. Williams, A. M. Smith, R. Collins, N. Hodson, A. K. Das and R. V. Ulijn 2009 Enzyme-assisted self-assembly under thermodynamic control. *Nature Nanotech.* **4**, 249-54.

[18] P. D. Josephy, T. Eling and R. P. Mason 1982 The horseradish peroxidase-catalyzed oxidation of 3,5,3',5'-tetramethylbenzidine. *J. Biol. Chem.* **257**, 3669-75.

[19] P. D. Josephy, R. P. Mason and T. Eling 1982 Cooxidation of the clinical reagent 3,5,3',5'-tetramethylbenzidine by prostaglandin synthase. *Cancer Res.* **42**, 2567-70.

[20] Z. Liu, M. Li, L. Turyanska, O. Makarovsky, A. Patanè, W. Wu and S. Mann 2010 Self-assembly of electrically conducting biopolymer thin films by cellulose regeneration in gold nanoparticle aqueous dispersions. *Chem. Mater.* **22**, 2675-80.

[21] L. Turyanska, O. Makarovsky, A. Patanè, N. V. Kozlova, Z. Liu, M. Li and S. Mann 2012 High magnetic field quantum transport in Au nanoparticle-cellulose films. *Nanotechnology* **23**, 045702.

[22] M. D. Backer and F. X. Sauvage 2007 *In situ* FTIR spectroelectrochemistry and spectral simulations using DFT: efficient complementary tools to elucidate complex electrochemical mechanisms. *J. Electroanal. Chem.* **602**, 131-7.

[23] M. Liu, Y. Zhang, Y. Chen, Q. Xie and S.Yao 2008 EQCM and *in situ* FTIR spectroelectrochemistry study on the electrochemical oxidation of TMB and the effect of large-sized anions. *J. Electroanal. Chem.* **622**, 184-92.

[24] A. S. Batsanov, P. J. Low and M. A. J. Paterson 2006 4,4'-diamino-2,2',6,6'-tetramethylbiphenyl. *Acta Crystallogr. Sect. E, Struct. Rep. Online* E62, o2973-5.

SOBRE EL ORGANIZADOR

El Dr. Juan Ramón Collet-Lacoste es licenciado en ciencias químicas de la Universidad de Buenos Aires (UBA) y PhD de la Universidad de Paris Sud (XI). Su especialidad es la físico química, en la rama de la termodinámica de los procesos irreversibles (TPI), especialmente en el estudio de los procesos cinéticos en los sistemas electroquímicos.

Ha desarrollado varios trabajos relacionados a los mecanismos de reacción y transporte de materia sobre electrodos metálicos, así como el desarrollo de electrodos para celdas de combustible de baja temperatura (fuel cells).

Es un especialista en la técnica de impedancia electroquímica, en la cual ha publicado varios artículos en revistas internacionales.

Desde el punto de vista experimental, ha trabajado en el desarrollo de celdas de combustible con Nps de platino y paladio y de electrolizadores alcalinos de baja temperatura.

Actualmente realiza trabajos sobre la oxidación acuosa del aluminio en gradientes de temperatura. Este trabajo esta relacionado a los elementos combustibles de los reactores experimentales multipropósito para la fabricación de radioisótopos de uso médico.

ÍNDICE REMISSIVO

T

V